Science & Technology Development Journal – Engineering and Technology, 4(SI2):SI38-SI46

Open Access Full Text Article

Research article

Analysis of the Stamping Speed for Sheet Metal Forming of Aluminum Alloy 5052-H112

Do Minh Dung[1,2], Vu Cong Hoa[1,2,*]

Use your smartphone to scan this QR code and download this article

ABSTRACT

Deep drawing is the most advanced sheet metal forming technique. In today's demanding environment is the global environment and energy saving, the process has been supposed to play a vital role in light-weight component industry. Light-weight, high strength, low density and extreme corrosion aspects must be almost guaranteed in a deep drawn product. However, due to those requirements, thinning and wrinkling and other defects will be increased also. Numerous elements such as blank-holder pressure, punch force, speed of punch, blank shape, thickness variation, surface-to-surface friction coefficient, material characteristic,…influenced to the success of methods as well as the quality of the products. In addition, worldwide manufacturers keep getting the most goods done in less time. Indeed, the increasing of productivity should be also dealt because it proportionally relates to the stamping speed. This paper investigates the influence of punch velocity on deformation behavior of aluminum alloy 5052–H112. Finite Element Method was used to perform Nakajima test at several of punch velocities of specimen widths and monitor fluctuations in magnitude of von Mises stress, the major strain and minor strain. Forming Limit Curve (FLC) was obtained at different velocities and almost uniform. Stretching and sliding across the top of the punch resulted in thinning of sheet metal. Beside this, the action of punch stroke resulted in the production of more von Mises concentrated stress and the largest specimen in widths had shown the peak value of von Mises stress compared with the other specimens at all different velocities. Furthermore, the ratio of the major strain to the minor strain is influenced by the mass of material at the contact area and keeps consistent over the variation in velocities of punch. This will pave the way for future studies of the optimization of the stamping speed in deep drawing.

Key words: Deep Drawing, Nakajima Test, Stamping Speed, Aluminum Alloy 5052, Forming Limit Curve (FLC)

[1]*Department of Engineering Mechanics, Faculty of Applied Sciences, Ho Chi Minh City University of Technology, 268 Ly Thuong Kiet Street, District 10, Ho Chi Minh City, Vietnam.*

[2]*Vietnam National University Ho Chi Minh City, Linh Trung Ward, Thu Duc District, Ho Chi Minh City, Vietnam.*

Correspondence

Vu Cong Hoa, Department of Engineering Mechanics, Faculty of Applied Sciences, Ho Chi Minh City University of Technology, 268 Ly Thuong Kiet Street, District 10, Ho Chi Minh City, Vietnam.

Vietnam National University Ho Chi Minh City, Linh Trung Ward, Thu Duc District, Ho Chi Minh City, Vietnam.

Email: vuconghoa@hcmut.edu.vn

History

- Received: 22-9-2021
- Accepted: 15-3-2022
- Published: 20-3-2022

DOI : 10.32508/stdjet.v4iSI2.922

Check for updates

INTRODUCTION

Regarding to the global environment and energetic issue, energy saving and safety have been properly thought out in automotive industry. Light-weight components of car are mostly made of sheet metal parts. Deep drawing plays a decisive role in sheet-forming process to produce these such parts. Indeed, the drawn part has been used not only in car but also aerospace, ship, drink and other fields [1,2]. Some of causes of this issue contain: punch force, holding force, speed of stamping, blank sheet geometry, variation in thickness, wrinkling, friction… [3,4]. Thus, it is an intrinsic to find out the process parameter which can lead defect-free product. To evaluate the formability of sheet metal in condition of bi-axial tension, Keeler proposed the idea of the Forming Limit Diagram (FLD) [5–8]. The Nakajima experiment is an approach to find out the Forming Limit Curve of sheet metal that based on the principle of deformation on blank sheet and combination of a lot kinds of testing specimens that was deformed by a hemispherical punch until detecting the fracture [9]. In a lot of findings belong to drawn part, researchers figured out holder force has a fairly functional in the forming ability of drawn parts [10]. Studying on minimum constant blank holder force to avoid wrinkling was proceeded by mathematical modeling, also be verified by Finite Element simulation [11]. Browne et al. [12] researches the variation and affect of die shape, punch, blank holder force, lubricating method and speed of stamping of C.R.1 steel cups in the deep drawing. Padmanabhan et al. [13] used Taguchi technique to investigate three factors: radius of die, blank-holding pressure and coefficient of friction in Finite Element method. Q. Bai et al. [14] conducted warm forming of aluminum alloy AA5754 at temperature from 200 to 300 degrees Celsius and at the stamping speed from 20 to 300 millimeter per second

In fact, relation between scrap rate and cycle time in production is inversely proportional and considering about the productivity is a common thread of manufactures in deep drawing field. The higher velocity

Cite this article : Dung D M, Hoa V C. **Analysis of the Stamping Speed for Sheet Metal Forming of Aluminum Alloy 5052-H112**. *Sci. Tech. Dev. J. – Engineering and Technology;* 4(SI2):SI38-SI46.

the better productivity and vise versa. Thus, in the present work, a velocity range of 10-120mm/s is discussed. The range is commonly used and magnitude of selected velocities is good enough to make deviation in results significantly. The object is to predict the Forming Limit Curve and to understand the effect of stamping speed on AA5052 at temper H112. The thickness is 1mm under deep drawing. Nakajima test was performed by Finite Element method at differences of the stamping speed and widths of specimen as shown in Figure 1.

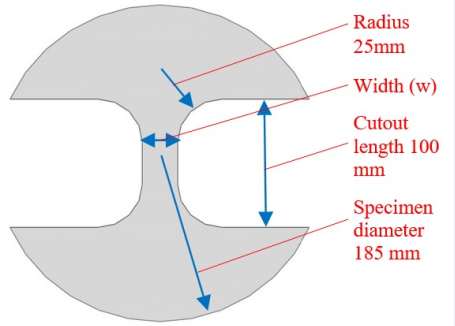

Figure 1: Specimen geometry

METHOLODOGY

Materials' Behavior

The isotropic hardening law is applied when doing the Finite Element method simulation. Power law relation governed material's behavior:

$$\sigma = K\varepsilon^n \quad (1)$$

where: n is strain hardening exponent, ε is true strain, K is strength coefficient, σ is true stress of the material.

Table 1 and Table 2 show the material properties and the chemical composition of AA5052-H112, respectively. Those specifications are followed a material certificate of a particular material lot of Russian manufacturer which conforms to all requirement of ASTM B209-14; SAE AMS-QQ-A-250/8 Rev. C (2014).

The true stress and true strain correlation of AA5052-H112 is shown in Figure 2.

Finite Element Modeling

The commercially available tool ABAQUS-Explicit was utilized to model the deep drawing procedure. The analysis was performed by using explicit FE approach. Tools included hemispherical punch (100mm diameter), blank holder and die (10mm radius fillet).

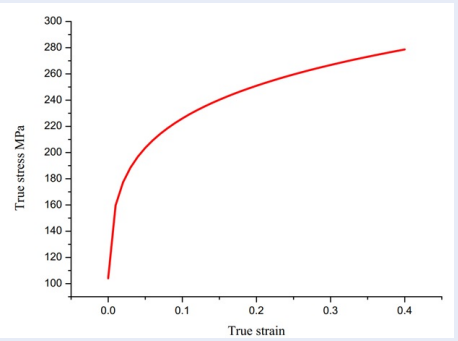

Figure 2: The true stress and true strain correlation of AA5052-H112

The set up of the simulation was performed on one haft sphere punch and different specimen widths at several of punch speeds that was clearly demonstrated in Figure 3. Deformation of punch, blank holder, die were disregarded, they were treated as rigid body. Deformable part is the blank sheet [15–17]. Solid homogeneous was used as element type of aluminum alloy 5052-H112. Friction has considered in simulation by using friction coefficient of 0.1 [10] applied to overall model, between tools and the blank sheet. Surface-to-surface contact was assigned for contacts in the whole deforming procedure of the assembly.

For meshing, a three dimensional element type C3D8R was chosen as element type of the blank sheet (an 8-node linear element, hourglass control reduced integration). For tools like punch, blank holder, die were used element type of R3D4 (a four- node 3-D bilinear rigid quadrilateral). Refer to Table 3 and Figure 4 for detail of elements used and element type assigning for each part.

In duration of deep drawing process, the parts such as punch, blank holder, die were constrained as fixed position while the unique vertical downward movement along to Z direction was applied to the blank sheet. Moreover, major strain and minor strain were monitored each time step of forming process for evaluation as the aim of the present study.

RESULTS AND DISCUSSION

Figure 5 demonstrated three dimensional stress state that was captured at the top of the punch for all specimen when they met the ultimate stress. There are no material constraints in the punch's direction, but there are in two other directions. That caused bending and sliding to have a significant influence on the sheet and compression had just a minor impact.

Table 1: Mechanical properties Of AA5052-H112

No.	Mechanical properties	Unit	Value
1	Mass density	kg/m^3	2680
2	Modulus of elasticity	GPa	70
3	Poisson's ratio	-	0.33
4	Strength coefficient	MPa	320
5	Work hardening coefficient	-	0.151
6	Tensile strength	ksi	28
7	Yield strength	ksi	15.2
8	Elongation	%	32.5
9	Hardness	HBW	58.9

Table 2: Chemical Composition Of AA5052-H112

No.	Chemical composition	Percentage %
1	Fe	0.26
2	Si	0.08
3	Cu	< 0.01
4	Mn	0.01
5	Mg	2.6
6	Cr	0.22
7	Zn	0.01
8	Al	remaining

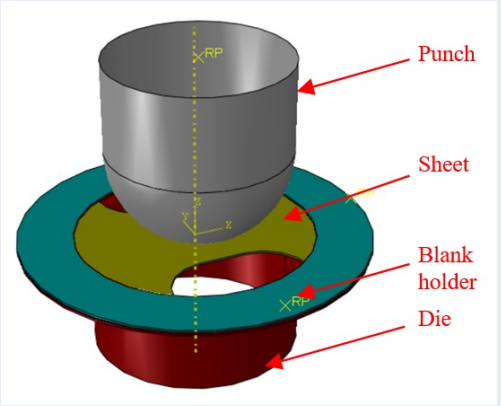

Figure 3: 3D model in simulation

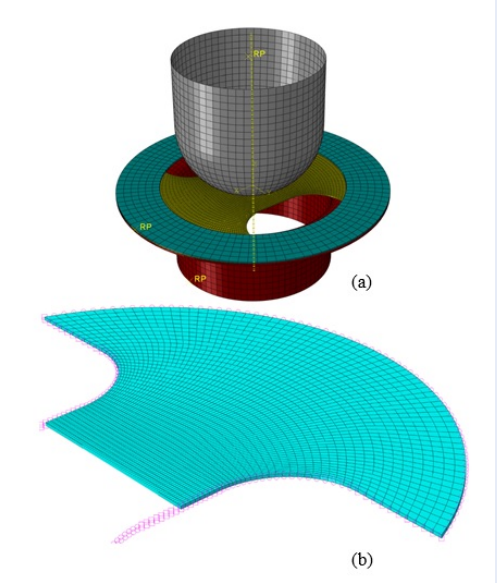

Figure 4: Meshing of FEM model (a) Mesh of overall entities; (b) Meshes of the blank sheet (cut in half)

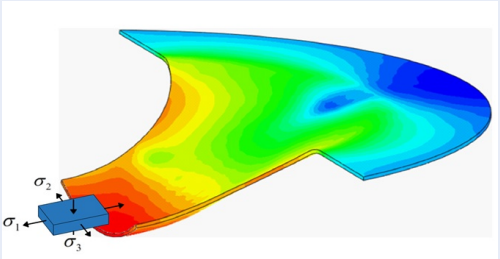

Figure 5: Stresses at the top of the punch

Table 3: Mesh properties

No.	Part	Element type	Element shape	Feature
1	Punch	R3D8	Quadrilateral	Rigid
2	Die	R3D8	Quadrilateral	Rigid
3	Holder	R3D8	Quadrilateral	Rigid
4	Sheet	C3D8R	Hexahedral	Solid

Thus, the sigma-1 was known as the major strain and the sigma-2 was known as the minor strain. In terms of magnitude, both of these dominated the sigma-3. Thinning of the drawn blank sheet's side-wall was caused by sliding and bending at the punch wall. More thinning also has made by sliding and stretching at the top of the punch. At the top of the punch, it is obvious that the maximum value of von Mises stress occurs for all situations. The comprehensive demonstration of the maximum value of von Mises stress at the punch top at variation specimen width range of 20-185mm and velocity of 10mm/s is mostly shown as Figure 6. In duration of deep drawing, the von Mises stress has a nonlinear increasing manner through the overall stroke of the punch. At the conclusion of the stroke, there is a steady rising tendency, but at the beginning of deep drawing process, von Mises stress displays a substantial increase in amplitude. Figure 7 clearly shown the tendency to growth of the stress of specimens. The tendency keeps consistent in through

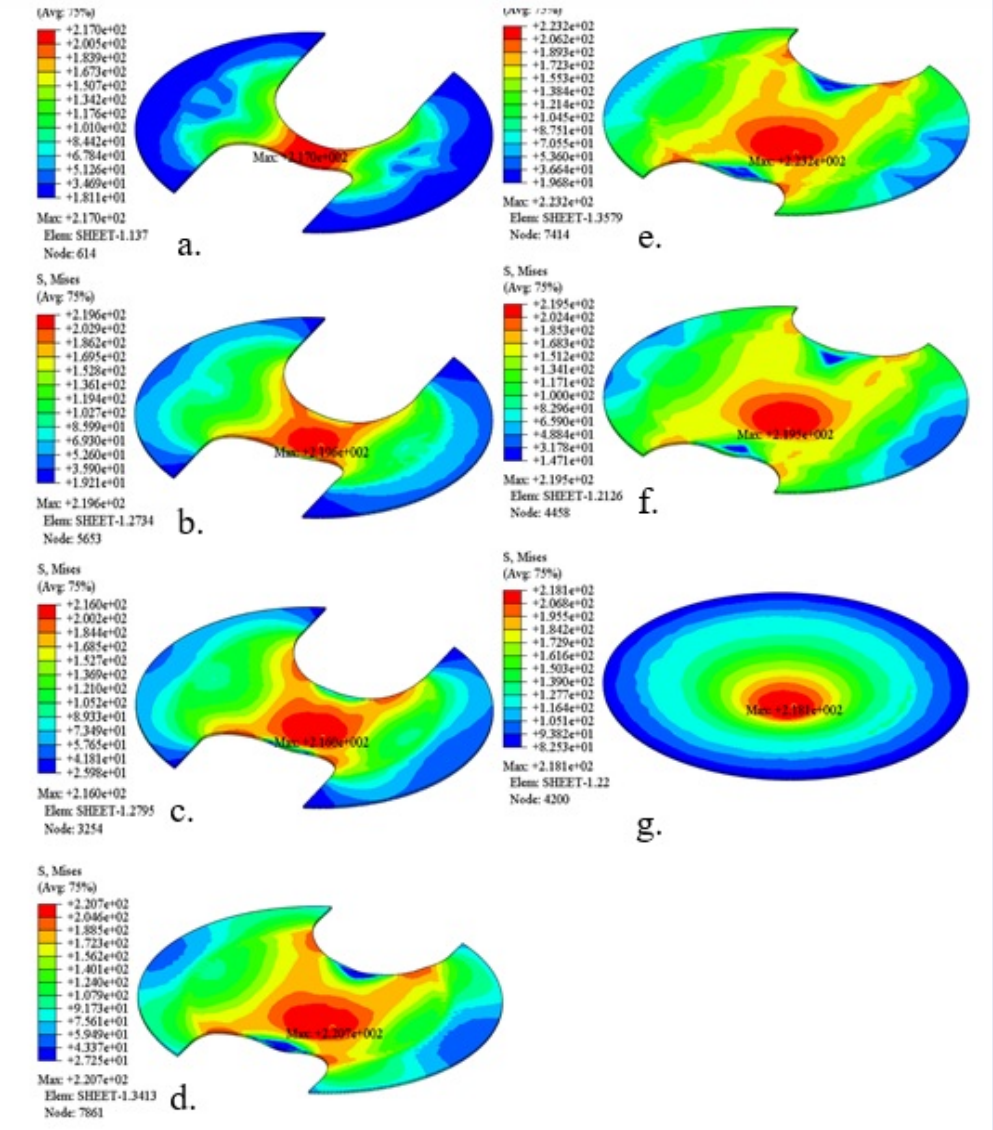

Figure 6: von Mises stress value of specimen widths at velocity of 10mm/s; (a) w=20; (b) w=40; (c) w=60; (d); w=90; (e) w=110; (f) w=135; (g) w=185

velocity range of 10-120mm/s. Maximum stress is formed at the summit as a result of maximum punch stroke. Comparing to the other specimens, the largest specimen 185mm had presented the highest value of von Mises stress.

It is apparent that maximum major strain occurs at the top of the punch at all situations, whereas the maximum minor strain happens at the R radius edges in smaller width specimens. The maximum minor strain increases substantially in wider width specimens at the top of the punch. Figure 10 depicts in detail the variation of the minor strain and the major of specimens at the greatest punch stroke. When the width of the specimen expands, the amplitude of the major strain drops while the amplitude of the minor strain increases. In conclusion, the length of the punch stroke has an effect on the strain. By monitoring the values of both the logarithmic minor strain and the logarithmic major strain during the deep drawing process, Forming Limit Curve (FLC) was completely obtained and shown as Figure 8 (the increasing of the width is from left to right). The values were acquired at the end of the procedure when the stress just met the ultimate stress of the material. The curves have a tendency to develop in the same way regardless of the velocity of the punch and clearly shown in Figure 9.

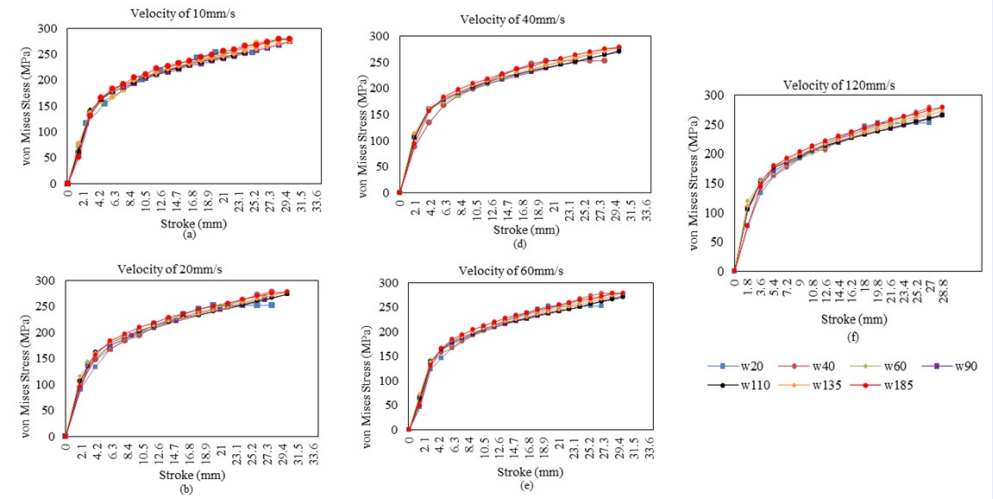

Figure 7: The von Mises stress at different velocities of specimens: a. 10 mm/s; b. 20 mm/s; c. 40 mm/s; d. 60 mm/s; e. 120 mm/s

Because of maximum punch stroke, maximum value of minor strain and maximum value of major strain develop at their apex.

In addition, the ratio of the logarithmic major strain to the logarithmic minor strain is demonstrated in Figure 9. There is a distinct ratio, the major strain divide to the minor strain, for each width of experiment pieces. These ratios are distributed around the ratio of the largest specimen (185mm). Two narrowest specimens, 20mm and 40mm in width, show negative ratios. The material in the center completely contacts the punch and there is less material in the center of the drawn parts that may cause the necking phenomena to occur and the drawn part to fail in this area. On the other side, three larger specimens (90mm, 110mm and 135mm in width) exhibit positive ratios. There is more material in the pressing area, it partially contacts the punch which allows for radial material stretching. In the final, the ratio converged at 1, the ratio of the largest specimen (185mm). All of ratios are nearly constant across the change in punch velocity using the Finite Element method. This will pave the way for studies of the optimization of the stamping speed in the deep drawing for the future of the present work. In general, the increasing of productivity should be dealt because it proportionally relates to stamping velocity. The optimization of stamping speed plays a vital role in increasing of productivity of the sheet metal forming industry.

CONCLUSION

The present study analyzed stamping speed for deep drawing of AA5052-H112. FE method was applied for specimens of the variation in widths that was suggested by Nakajima test. Also, many of velocities were performed, from 10mm/s to 120mm/s. The followings are conclusions of the study:

1. Sliding and stretching at the punch's top caused thinning in this area. The sigma-3 was dominated by the major strain (sigma-1) and the minor strain (sigma-2).
2. The effect of punch stroke resulted in the production of more von Mises stress within specimens.
3. The concentration of stress occurred at the top of the punch in during of deep drawing process until the stress reaches the ultimate stress of the material.
4. The increasing manner of stress was non-linear. A gradually upward trend was shown in the end of the punch travel while the stress shown a significant surge in magnitude in the onset the process.
5. Comparing to the other specimens, the largest specimen 185mm had presented the highest value of von Mises stress in all stamping speeds.
6. The amplitude of the major strain decreases as the specimen's breadth grows, while the amplitude of the minor strain increases.
7. At varying velocities, the FLC was nearly uniform.
8. The mass of material at the contact area might lead to negative ratio or positive ratio, the major strain divide to the minor strain.

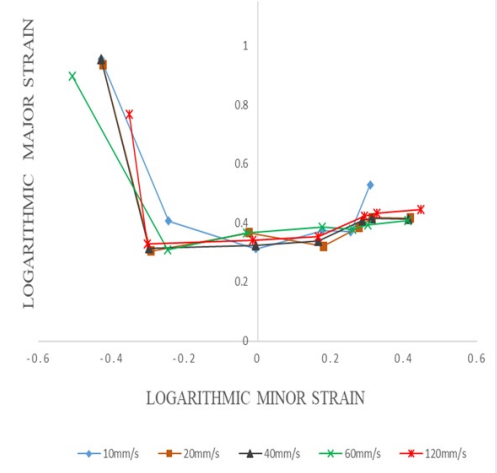

Figure 8: Forming Limit Curve of AA5052-H112

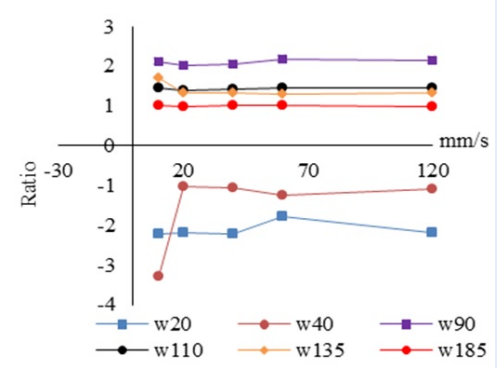

Figure 9: The ratio strain

9. The ratio of the major strain to the minor strain keeps consistent through the variation in stamping speeds.

ACKNOWLEDGMENT

We appreciate the support from Ho Chi Minh City University of Technology (HCMUT), VNU-HCM for the present study.

NOMENCLATURES

FLC: Forming Limit Curve
FLD: Forming Limit Diagram
FE: Finite element

CONFLICT OF INTEREST

There is no any conflict of interest in publishing the present paper. Authors group has an agreement that this manuscript is original and has not been published before.

AUTHOR CONTRIBUTION

Do Minh Dung is as the core developer of the approach of research, gathering data and the manuscript editor.

Vu Cong Hoa is as the supervisor, brainstorms concepts for the method proposed and also involves in checking the data and simulation results and manuscript.

REFERENCES

1. Reddy ACS, et al. An experimental study on effect of process parameters in deep drawing using Taguchi technique. International Journal of Engineering, Science and Technology, vol. 7, no. 1, pp. 21-32, 2015;Available from: https://doi.org/10.4314/ijest.v7i1.3.
2. Mugendiran V, et al. Tensile Behaviour of Al5052 Alloy Sheets Annealed at Different Temperatures. Advanced Materials Research, vol. 845, pp. 431-435, 2015;Available from: https://doi.org/10.4028/www.scientific.net/AMR.845.431.

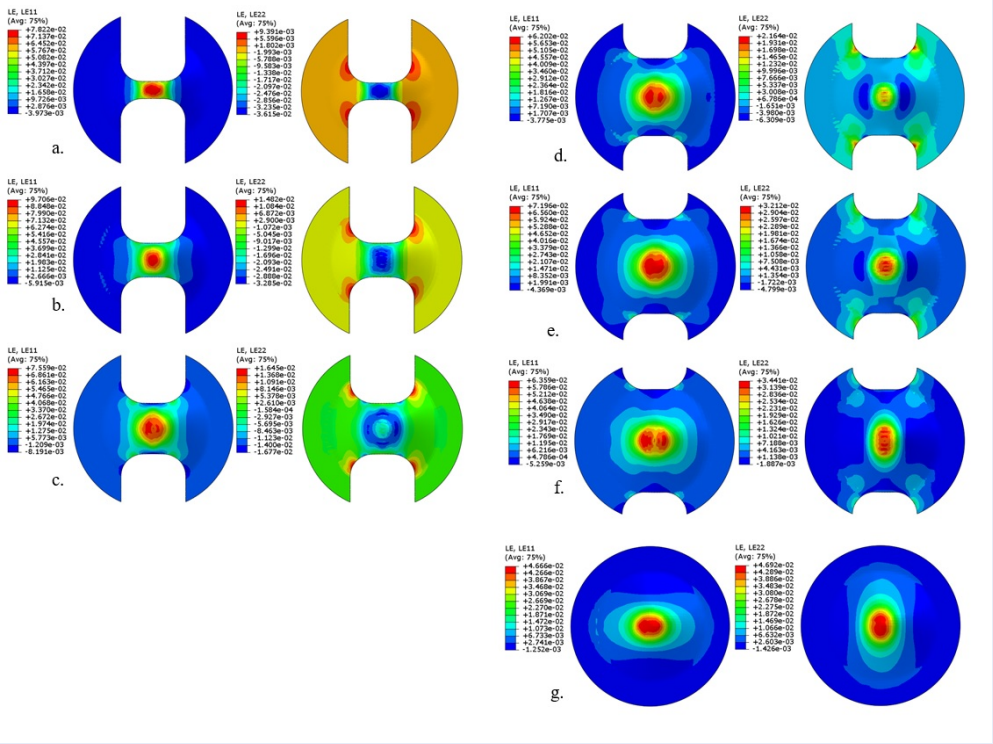

Figure 10: The major strain (left) and the minor strain (right) of specimen at velocity of 120mm/s: (a) w=20; (b) w=40; (c) w=60; (d); w=90; (e) w=110; (f) w=135; (g) w=185

3. Tian L, et al. Optimization of Process Parameters in Deep Drawing Process Based on Orthogonal Experiment Method," 3rd International Conference on Mechanical Engineering and Intelligent Systems, pp. 684-688, 2015;Available from: https://doi.org/10.2991/icmeis-15.2015.127.
4. Singh CP, Agnihotri G. Study of Deep Drawing Process Parameters: A Review. International Journal of Scientific and Research Publications, vol. 5, no. 2, pp. 1-15, 2015;.
5. dos Santos Freitas MC, et al. Experimental Analysis and Theoretical Predictions of the Limit Strains of a Hot-dip Galvanized Interstitial-free Steel Sheet. Materials Research, vol. 16, no. 2, pp. 351-366, 2013;Available from: https://doi.org/10.1590/S1516-14392013005000015.
6. Kumar SD, et al. Development of Nakazima Test Simulation Tool for Forming Limit Diagram Generation of Aluminium Alloys. International Journal of Engineering Studies and Technical Approach, vol. 01, no. 10, pp. 37-45, 2015.;.
7. Gatea S, et al. Evaluation of formability and fracture of pure titanium in incremental sheet forming. Int J Adv Manuf Technol , vol. 95, pp. 625-641, 2018;Available from: https://doi.org/10.1007/s00170-017-1195-z.
8. Djavanroodi F, Derogar A. Experimental and numerical evaluation of forming limit diagram for Ti6Al4V titanium and Al6061-T6 aluminum alloys sheets. Materials and Design. 2012;31:4866–4875. Available from: https://doi.org/10.1016/j.matdes.2010.05.030.
9. Schwindt CD, et al. Forming Limit Curve Determination of a DP-780 Steel Sheet. Procedia Materials Scienc, vol. 8, pp. 978-985, 2015;Available from: https://doi.org/10.1016/j.mspro.2015.04.159.
10. Dewang Y, et al. Influence of Punch Velocity on Deformation Behavior in Deep Drawing of Aluminum Alloy," ASM International, 2020;Available from: https://doi.org/10.1007/s11668-020-01084-5.
11. Candra S, et al. Modeling of the minimum variable blank holder force based on forming limit diagram (FLD) in deep drawing process," IOP Conf. Series: Materials Science and Engineering, vol. 273, 2017;Available from: https://doi.org/10.1088/1757-899X/245/1/012014.
12. Browne MT, Hillery MT. Optimising the variables when deep-drawing C.R.1 cups. Journal of Materials Processing Technology, vol. 136, pp. 64-71, 2003;Available from: https://doi.org/10.1016/S0924-0136(02)00934-2.
13. Padmanabhana R, et al. Influence of process parameters on the deep drawing of stainless steel. Finite Elements in Analysis and Design , vol. 43, pp. 1062-1067, 2007;Available from: https://doi.org/10.1016/j.finel.2007.06.011.
14. Shao Z, et al. Experimental investigation of forming limit curves and deformation features in warm forming of an aluminium alloy. Journal of Engineering Manufacture, vol. 232, no. 3, pp. 465-474, 2016;Available from: https://doi.org/10.1177/0954405416645776.
15. Daxin E, Takaji Mizuno, Zhiguo Li. Stress analysis of rectangular cup drawing. Jurnal of Materials Processing Technology, vol. 205, pp. 469-476, 2008;Available from: https://doi.org/10.1016/j.jmatprotec.2007.11.274.
16. Karajibani E, et al. Forming limit diagram of aluminum-copper two-layer sheets: numerical simulations and experimental verifications. Int J Adv Manuf Technol, 2016;Available from: https://doi.org/10.1007/s00170-016-9585-1.
17. Kami A, et al. Numerical determination of the forming limit curves of anisotropic sheet metals using GTN damage model. Journal of Materials Processing Technology, vol. 216, pp. 472-483, 2015;Available from: https://doi.org/10.1016/j.jmatprotec.2014.10.017.

Tạp chí Phát triển Khoa học và Công nghệ – Engineering and Technology, 4(SI2):SI38-SI46

Open Access Full Text Article

Bài nghiên cứu

Phân tích tốc độ dập để tạo hình kim loại tấm bằng hợp kim nhôm 5052-H112

Đỗ Minh Dũng[1,2], Vũ Công Hòa[1,2,*]

Use your smartphone to scan this QR code and download this article

TÓM TẮT

Dập sâu là một trong các hương pháp gia công kim loại tấm tiên tiến nhất. Ngày nay, yêu cầu khắc khe của môi trường là vấn đề môi trường toàn cầu và tiết kiệm năng lượng, quy trình này đã và đang được đánh giá là không thể thiếu trong ngành công nghiệp linh kiện trọng lượng nhẹ. Các khía cạnh như khối lượng nhẹ, đảm bảo độ bền, mật độ thấp và có khả năng chống ăn mòn cao hầu như phải được đảm bảo trong một sản phẩm dập sâu. Tuy nhiên, do những yêu cầu đó mà độ mỏng thành, xuất hiện các nếp nhăn và các khuyết tật khác sẽ gia tăng. Sự thành công của phương pháp, cũng như chất lượng của sản phẩm, sẽ chịu ảnh hưởng từ nhiều yếu tố, có thể kể đến như lực ép lên bộ phận giữ phôi, lực dập, tốc độ dập, hình dạng phôi tấm, độ dày tấm kim loại, hệ số ma sát giữa các bề mặt, đặc tính vật liệu,… Hơn nữa, các nhà sản xuất trên toàn thế giới luôn luôn cố gắng nâng cao sản xuất bằng cách trong thời gian ngắn nhất nhưng tạo ra nhiều sản phẩm nhất. Thật vậy, việc tăng năng suất cần phải được giải quyết vì nó tỷ lệ thuận với tốc độ dập trong quá trình sản xuất. Nghiên cứu này sẽ trình bày ảnh hưởng của vận tốc dập đến ứng xử biến dạng của hợp kim nhôm 5052 – H112, sử dụng phương pháp phần tử hữu hạn để thực hiện thí nghiệm theo mô hình Nakajima ở một số vận tốc dập kết hợp với sự thay đổi bề rộng của mẫu thử và khảo sát sự dao động về ứng suất von Mises, biến dạng chính và biến dạng phụ. Đường cong giới hạn gia công (FLC) thu được ở các vận tốc khác nhau và gần như đồng nhất. Việc kéo căng và trượt ở phần đỉnh của chày dẫn đến việc tấm kim loại bị mỏng đi. Bên cạnh đó, sự tác động của chày dẫn đến việc tập trung ứng suất von Mises và mẫu thử có kích thước chiều rộng lớn nhất cho thấy giá trị đỉnh của ứng suất von Mises so với các mẫu khác ở tất cả các vận tốc khác nhau. Hơn nữa, tỷ lệ giữa biến dạng chính và biến dạng phụ bị ảnh hưởng bởi khối lượng vật liệu tại khu vực tiếp xúc và luôn nhất quán với sự thay đổi vận tốc của chày. Kết luận này sẽ mở đường cho các nhiệm vụ sắp tới về việc tối ưu hóa tốc độ dập trong lĩnh vực dập sâu.

Từ khoá: Dập sâu, Thí nghiệm Nakajima, Tốc độ dập, Hợp kim nhôm 5052, Đường công giới hạn gia công (FLC)

[1]*Bộ môn Cơ Kỹ Thuật, Khoa Khoa Học Ứng Dụng, Trường Đại Học Bách Khoa, 268 Lý Thường Kiệt, Quận 10, Thành phố Hồ Chí Minh.*

[2]*Đại Học Quốc Gia Thành Phố Hồ Chí Minh, Linh Trung, Thủ Đức, TP.HCM*

Liên hệ

Vũ Công Hòa, Bộ môn Cơ Kỹ Thuật, Khoa Khoa Học Ứng Dụng, Trường Đại Học Bách Khoa, 268 Lý Thường Kiệt, Quận 10, Thành phố Hồ Chí Minh.

Đại Học Quốc Gia Thành Phố Hồ Chí Minh, Linh Trung, Thủ Đức, TP.HCM

Email: vuconghoa@hcmut.edu.vn

Lịch sử

- Ngày nhận: 22-9-2021
- Ngày chấp nhận: 15-3-2022
- Ngày đăng: 20-3-2022

DOI : 10.32508/stdjet.v4iSI2.922

Check for updates

Trích dẫn bài báo này: Dũng D M, Hòa V C. **Phân tích tốc độ dập để tạo hình kim loại tấm bằng hợp kim nhôm 5052-H112**. *Sci. Tech. Dev. J. - Eng. Tech.;* 4(SI2):SI38-SI46.